RSC Advances

PAPER

View Article Online
View Journal | View Issue

Cite this: *RSC Adv.*, 2026, **16**, 16661

Sustainable utilization of waste expanded polystyrene in cellulose acetate polymer blend membranes for CO_2/CH_4 separation

Bharat Nayak, Maulik Gauswami and Bhanu Vardhan Reddy Kuncharam *

Expanded polystyrene (EPS) commonly called thermocol is a widely used packaging material that poses serious environmental challenges due to its poor biodegradability and low recycling. This study investigates the use of waste EPS to develop sustainable polymer blend membranes using cellulose acetate (CA) *via* solution casting and solvent evaporation technique for carbon dioxide (CO_2) separation. The membranes were characterized using fourier transform infrared spectroscopy (FTIR), X-ray diffraction (XRD), differential scanning calorimetry (DSC), and field-emission scanning electron microscopy (FESEM) techniques. Model biogas having CO_2/CH_4 composition of 40 : 60 was used to test blend membranes at 1.5 and 3 bars. A significant enhancement in the CO_2 permeability was observed after the incorporation of EPS due to increased chain flexibility and free volume. The 5 wt% EPS/CA blend membrane showed the highest CO_2 permeability of 105.83 Barrer with 15.98 CO_2/CH_4 selectivity at 3 bar. 10 wt% EPS loaded blend membrane achieved the highest CO_2/CH_4 selectivity of 21.25 with 47.63 Barrer CO_2 permeability at 1.5 bar. The results have demonstrated that blending of CA with waste EPS is an effective strategy that can upcycle plastic waste into value added membrane material which can be used for efficient CO_2 separation and sustainable biogas upgrading.

Received 17th February 2026
Accepted 18th March 2026

DOI: 10.1039/d6ra01412g

rsc.li/rsc-advances

1 Introduction

The growing problem of plastic waste is a major global environmental challenge.[1] Expanded polystyrene (EPS) commonly known as Thermocol is a lightweight, rigid, and thermoplastic polymer commonly used in packaging, insulation, and disposable products. Despite its significant usage, EPS is non-biodegradable and has a very low recycling rate which is a serious environmental issue.[2] After usage in large quantities EPS is directly dumped into the landfills and water bodies which contribute to the pollution and ecological damage.

Traditional recycling techniques for EPS are limited and require high cost and complex logistics which may also reduce its mechanical properties after reprocessing. Valorizing EPS waste into value-added products provides a dual benefit in response to the increasing global emphasis on circular economy and sustainability: it reduces plastic waste and generates functional materials.[3] Santana-Luna *et al.* have developed a series of asymmetric membranes based on EPS waste by phase inversion for water treatment through direct sulfonation.[4] The sulfonic acid groups increased the membranes hydrophilicity due to which the overall permeability and dye rejection capability of the membranes has improved.

Department of Chemical Engineering, Birla Institute of Technology and Science Pilani, Pilani, Rajasthan, 333031, India. E-mail: bhanu.vardhan@pilani.bits-pilani.ac.in; Tel: +91-1596255839

Biogas is a renewable energy source primarily produced through the anaerobic digestion of organic waste. The raw biogas typically contains 35–50% CO_2, which is inert and non-combustible and decreases its calorific value and poses corrosion risks to pipelines and end-use equipment. Efficient purification techniques are required to enhance the CH_4 concentration in biogas to make it suitable for energy applications, particularly as a vehicle fuel or for grid injection.[5,6] Therefore, removing CO_2 is a crucial step for enhancing biogas. Existing CO_2 separation techniques are chemically aggressive, economically unsustainable and require lots of energy and space (*e.g.* chemical absorption, amine scrubbing, pressure swing adsorption, and cryogenic separation).[7–9] Membrane based gas separation has become a viable, adaptable, and environmentally friendly substitute for conventional purifying methods in this regard. Membrane based separation systems operate under relatively mild conditions, require minimal chemical input, and are easily scalable.[10]

Over the years extensive research has been conducted on polymeric membrane materials; such as polyvinylidene fluoride (PVDF), polysulfone (PSF), polyethersulfone (PES), polyacrylonitrile (PAN), polyimide (PI), polyetherimide (PEI), polyvinyl alcohol (PVA), cellulose acetate (CA) and more.[11–13] Amongst the different polymers reviewed, cellulose acetate (CA) has attracted plenty of interest due to its processability, biocompatibility and moderate gas separation capability.[14–16] Different inorganic filler materials such as metal organic

frameworks (MOFs), zeolites and carbon based materials have been added to CA for improving its gas separations capacity. The technique of mixing inorganic filler into polymer is called mixed matrix membranes (MMMs) technique.[17] The fabrication processes of MMMs is complex which result in interfacial defects and limits long-term stability in industrial conditions. Such issues affect the membrane's gas separation capability, durability and commercial viability.[18]

Polymer blending is another effective strategy which can improve membrane performance. This technique allows modification of the physical, mechanical, and transport properties of polymer material by incorporating different polymeric phases. Neves *et al.* have mixed PEI and PES polymers in varying ratios to prepare carbon molecular sieve membranes.[19] Nayak *et al.* mixed CA and PI polymers for CO_2 separation and achieved 9.4 CO_2/CH_4 selectivity.[20] Payami *et al.* blended polysulfone and poly(butylene succinate) (PBS) using the solution casting and solvent evaporation method. It was noticed that with the 5% and 10% blend ratios, the CO_2/CH_4 selectivity increased by 187% and 43%, respectively, along with notable enhancements in pure CO_2 permeance.[21] Therefore, by blending technique polymeric membranes can be engineered to selectively permit the specific gases, making them suitable for CO_2/CH_4 separation.

Blending waste EPS with the other polymers such as CA for the membrane development may represent an innovative upcycling approach that aligns with current environmental, economic, and technological needs. Waste EPS is primarily composed of polystyrene (PS), possesses high rigidity, hydrophobicity, and good film-forming potential, which can synergistically enhance the properties of CA-based membranes. Extensive research has been conducted on MMMs containing nanomaterials or functional fillers; very few studies have explored polymer blend systems using waste-derived components.[22]

Therefore, here in this study, we have fabricated polymer blend membranes using cellulose acetate and waste EPS by one step solution casting and solvent evaporation technique. The membranes were tested with the model biogas at two different pressures. Analytical techniques such as fourier transform infrared spectroscopy (FTIR), thermogravimetric analysis (TGA), differential scanning calorimetry (DSC), X-ray diffraction (XRD), and field-emission scanning electron microscopy (FESEM) were used for characterization. The integration of CA with waste EPS offers a novel approach for producing blend membranes that combines the CO_2 affinity of CA with the mechanical and morphological properties of polystyrene. The incorporation of waste EPS adds a sustainability aspect and offers a method to reduce plastic waste and dependency on virgin raw materials. The differences in polymer solubility might lead to microstructural changes, including improved free volume or microphase separation, which could enhance gas transport properties and make the membranes suitable for extensive biogas upgrading applications.

In this work, sustainable strategy for valorizing waste expanded polystyrene (EPS) by incorporating it into cellulose acetate (CA) polymer matrices for fabrication of gas separation membranes is reported. The study aims to investigate the feasibility of utilizing waste EPS as a polymer blending component to modify membrane structure and gas transport behavior.

As polystyrene has previously been explored in membrane materials for other applications. To the best of our knowledge there are no reports on the use of waste derived EPS blended with cellulose acetate for CO_2/CH_4 gas separation membranes. To the best of our knowledge this is the first study on utilizing waste EPS as a polymeric component for biogas upgrading membranes. The incorporation of waste EPS into CA polymer matrix for gas separation is a relatively unknown process that will open up new possibilities for membrane research and the upcycling of plastic waste.

2 Experimental

2.1 Materials

Expanded polystyrene was recovered from electronic packaging waste. Cellulose acetate (average M_n ~50 000, acetyl content ~38–40 wt%) was procured from Simson pharma limited, India. *N*,*N*′ dimethylformamide (DMF 99.5%) was purchased from Merck, India. All the chemicals were used as purchased.

2.2 Membrane preparation

The process of the membrane preparation is shown in Fig. 1 neat CA and EPS/CA blend membranes were prepared by varying the weight fraction of EPS (1, 5, and 10 wt%). The EPS weight percentage (wt%) in EPS/CA blend was calculated using eqn (1):

$$\text{Wt\% of EPS} = \frac{W_{EPS}}{W_{CA} + W_{EPS}} \times 100 \quad (1)$$

Here, W_{EPS} is weight of EPS in grams and W_{CA} is weight of CA in grams.

2.3 Neat CA membrane preparation

Initially, CA flakes (18 wt%) were weighed and dried in an air oven at 100 °C for 3–4 h to eliminate residual moisture. The dried CA flakes were then slowly added to 30 ml DMF solvent and continuously stirred overnight using a magnetic stirrer at approximately 500 rpm at room temperature (~25 °C) until a homogenous solution was obtained. The resulting polymer solution was then sonicated in an ultrasonic bath (40) kHz for 30 min to eliminate any polymer agglomerates and then degassed for 1 h under ambient conditions to remove entrapped air bubbles.

For membrane casting, the degassed polymer solution was poured onto a clean dust-free flat glass plate. The film was uniformly spread using a straight glass rod by sliding from top to bottom of the plate to ensure consistent thickness. The cast film was then placed in a vacuum oven and dried at 60 °C to facilitate slow solvent evaporation. Drying was continued until complete solvent evaporate which allows the membrane detach naturally from the glass plate indicates complete drying.

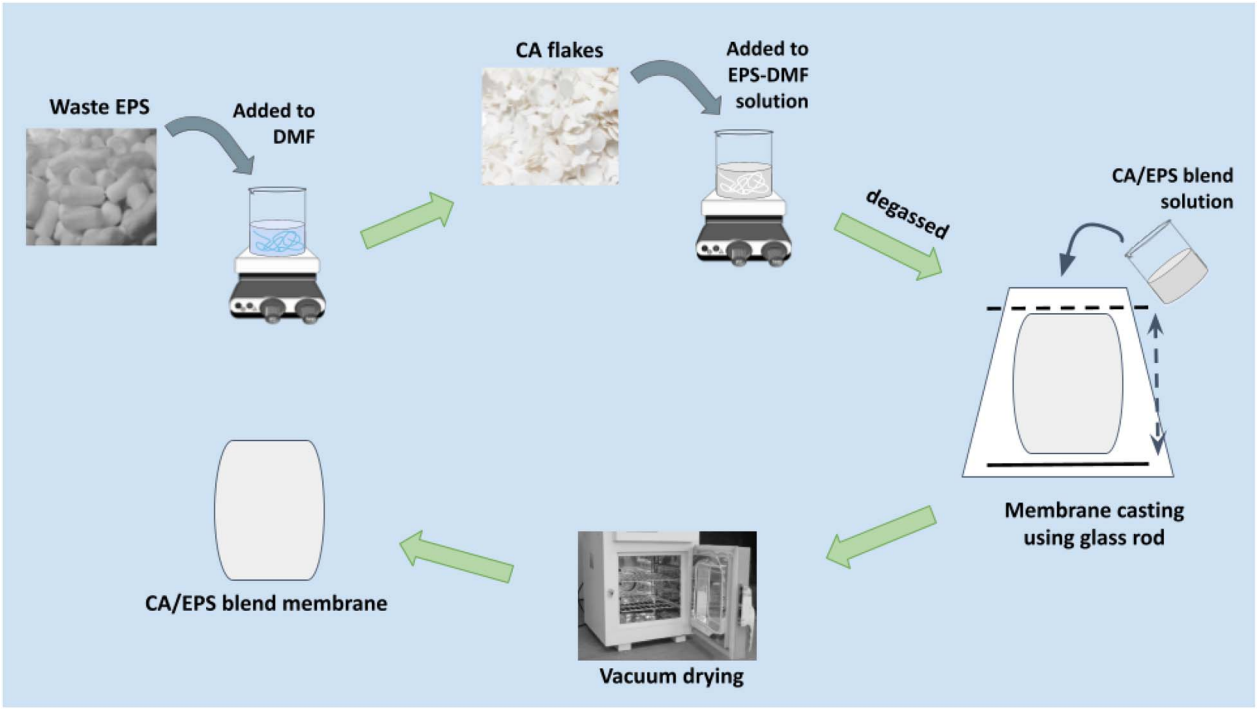

Fig. 1 Schematic illustration of EPS/CA blends membranes preparation.

2.4 EPS/CA blend membrane preparation

For the synthesis of EPS/CA blend membranes, waste EPS was first washed thoroughly with deionized water to remove any surface impurities and dried in an air oven at 40 °C. A pre-calculated amount of EPS (corresponding to desired blend ratio) was then dissolved into 30 ml DMF under continuous stirring until clear solution was obtained. And then the required amount of CA flakes maintaining 18 wt% total polymers content (CA + EPS for blend membranes) was added to the EPS-DMF solution and stirred overnight under similar conditions as those used for neat CA membranes. The obtained homogenous polymer solution was then subjected to sonication and degassing followed by casting and drying using the same procedure as used for the neat CA membrane.

2.5 Membrane characterization

Tensile strength of the neat CA and EPS/CA blend membranes were carried out using Single column Universal Testing Machine (UTM, Instron 34SC-5, USA). The membranes having length of 150 mm and width of 30 mm was fixed vertically. Then the membrane sample was extended at a constant displacement rate 10 mm min^{-1} until it was broken. The average tensile strength of at least three membranes was taken for each membrane type. Structural analysis of the membranes was done using X-ray diffraction (XRD, Bruker D8 Advance, Germany) equipped with Cu Kα radiation (λ = 0.154 nm). Scans were recorded over a 2θ range of 5°–60° with the scanning rate of 2° min^{-1}. Functional group analysis was performed using fourier transform infrared spectroscopy (FTIR, PerkinElmer Frontier, USA) by forming potassium bromide (KBr) pellets in a hydraulic press under 10 tons of pressure. The spectra were acquired over the wavenumber range of 4000–500 cm^{-1} at resolution of 10 cm^{-1}. Thermal behavior and glass transition temperature (T_g) analysis of the membranes was carried out using differential scanning calorimetry (DSC, PerkinElmer DSC-4000, USA). The surface morphology of the membranes was examined using field emission electron microscopy (FESEM, FEI Apreo LoVac model). Membrane samples were sputter-coated over double sided carbon tape with a thin layer of gold to enhance surface conductivity and image clarity.

2.6 Evaluation of gas permeation and separation performance

Gas permeation experiments were conducted at 25 °C to assess the transport behavior of CO_2 and CH_4 through neat CA and EPS/CA blend membranes at pressures of 1.5 and 3 bar. A biogas mixture with a composition of CO_2 and CH_4 in a 40 : 60 ratio was used as the feed gas. The composition of the outlet gas was determined with a gas chromatograph (GC, Shimadzu GC-2014, Japan) that consisted of a thermal conductivity detector (TCD) and shincarbon packed column was operated using LabSolutions software. Using a digital micrometre, the membrane's average thickness was calculated (present in SI), for each membrane sample at least five measurements were taken at different positions and the average thickness along with standard deviation was calculated. A detailed discussion and systematic schematic of the gas permeation setup is present in the Fig. S3 in SI. When the EPS loading increased up to 10% or more it was observed that the flexibility of blend membranes reduces which means higher EPS loading lead to noticeable

stiffness and brittleness due to the rigid nature of polystyrene segments.

The mixed gas permeability and their selectivity were calculated using eqn (2) and (3):[10,23]

$$P = \frac{q \cdot \delta}{A \cdot \Delta p} \quad (2)$$

$$\alpha_{CO_2/CH_4} = \frac{P_{CO_2}}{P_{CH_4}} \quad (3)$$

where, P represents permeability measured in Barrers, δ represents the membrane thickness in cm while Δp represents the partial pressure difference across the membrane in cm Hg, A represents the membrane's effective area, and α represents the selectivity measured from the ratio of permeability of CO_2 and CH_4. Although the pressure values in the experiments are reported in bar, the permeability calculation follows the conventional Barrer definition where pressure difference (Δp) is expressed in cm Hg.

3 Results and discussion

3.1 Viscosity measurements

The rheological behavior of the neat CA and EPS/CA blends casting solutions was measured using digital Labtronics viscometer at rotational speed of 6 rpm. The obtained viscosity values of neat CA, 1 wt%, 5 wt%, and 10 wt% EPS loaded CA solution were plotted in Fig. 2. It was observed that viscosity of the solutions increased with the increase in EPS loading. The neat CA solution exhibited viscosity of 6039 mPa.s whereas EPS/CA blend solutions showed higher viscosity values reaching up to 8555 mPa s^{-1} for 10 wt% EPS/CA blend. This increase in viscosity is due to EPS chains and their interaction with CA matrix which increases the resistance to flow in the casting solution. Fully miscible blends shows linear type of curve and partially miscible blends shows non-linear curve. Whereas, fully immiscible blends shows S-segment or S-shaped curve.[24] From Fig. 2, it was observed that EPS/CA blends system is immiscible. Higher viscosity can limit polymer chain mobility during solvent evaporation and film formation which may influence the polymer chain packing and thereby affect membrane morphology and gas transport properties.

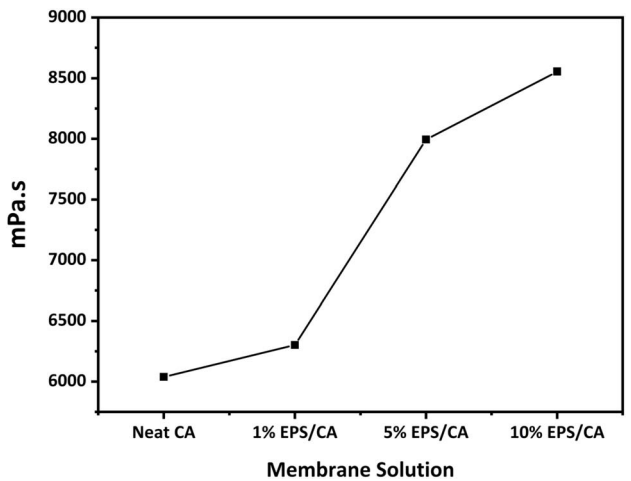

Fig. 2 Shear viscosity of neat CA, and EPS/CA blend systems of different EPS weight ratios.

3.2 FTIR analysis

Functional group analysis of neat CA, EPS, and EPS/CA blend membranes with 1, 5, and 10% EPS loadings was done using FTIR spectroscopy (Fig. 3). In the FTIR spectrum of neat CA a broad peak was observed around 3455 cm^{-1} which is attributed to stretching vibration of hydroxyl (–OH) groups. At 2941 cm^{-1}, an aliphatic –CH stretching peak was also observed. A sharp peak at 1769 cm^{-1} was observed which is a corresponding peak of stretching vibration of the carbonyl (C═O) group. The stretching band at 1384 cm^{-1} was due to symmetric deformation of CH groups. At 1270 cm^{-1} and 1040 cm^{-1} two peaks were seen due to stretching vibrations of C–C–O and C–O groups, confirming the presence of ester linkages in the polymer backbone of CA.[25]

The FTIR spectrum of EPS has shown similar peaks to polymer structure of styrene. The two adsorption peaks around 3101 cm^{-1} and 2999 cm^{-1} were raised due to stretching vibrations of CH group from the aromatic rings. Peaks at 2919 cm^{-1} and 2848 cm^{-1} correspond to stretching vibration of C–H groups from the polymer backbone. Stretching vibrations of aromatic C–C are evident at 1599 cm^{-1} and 1454 cm^{-1}. At 768 cm^{-1} and 704 cm^{-1}, out of plane C–H bending vibrations appeared that represent the characteristic fingerprint of polystyrene structure.[26]

The overall spectra of EPS/CA blend membranes follow the spectra of CA. At lower loading of 1% EPS, the spectra retained dominant CA peaks with lower intensity of –OH stretching band at 3455 cm^{-1} suggesting weak physical–physical interactions or partial hydrogen bonding between CA and EPS. When the loading is increased to 5% and 10% two aromatic characteristic peaks of EPS at 1599 cm^{-1} and 1454 cm^{-1} become prominent. A marginal shift in carbonyl peak was observed at ~1772 cm^{-1} in CA/EPS blend membranes which show weak intermolecular interactions between the CA matrix and aromatic rings of EPS. The –C═O stretching peak of CA shifts from ~1769 cm^{-1} to ~1772 cm^{-1}, decrease intensity –OH stretching band indicates reduced hydrogen bonding within the CA matrix. These observed spectral changes suggest weak intermolecular interactions between CA and EPS that may be through dipole–π interactions between acetyl groups and aromatic rings of polystyrene. These interactions influence polymer chain packing and contribute to the observed increase in free volume.

The presence of collective peaks of both CA and EPS in the spectra of the blend membranes confirms the formation of EPS/CA blend.

3.3 XRD analysis

To investigate the structural characteristics of the membranes X-ray diffraction (XRD) technique was used. The XRD pattern of neat CA, EPS, and EPS/CA blend membranes with different EPS

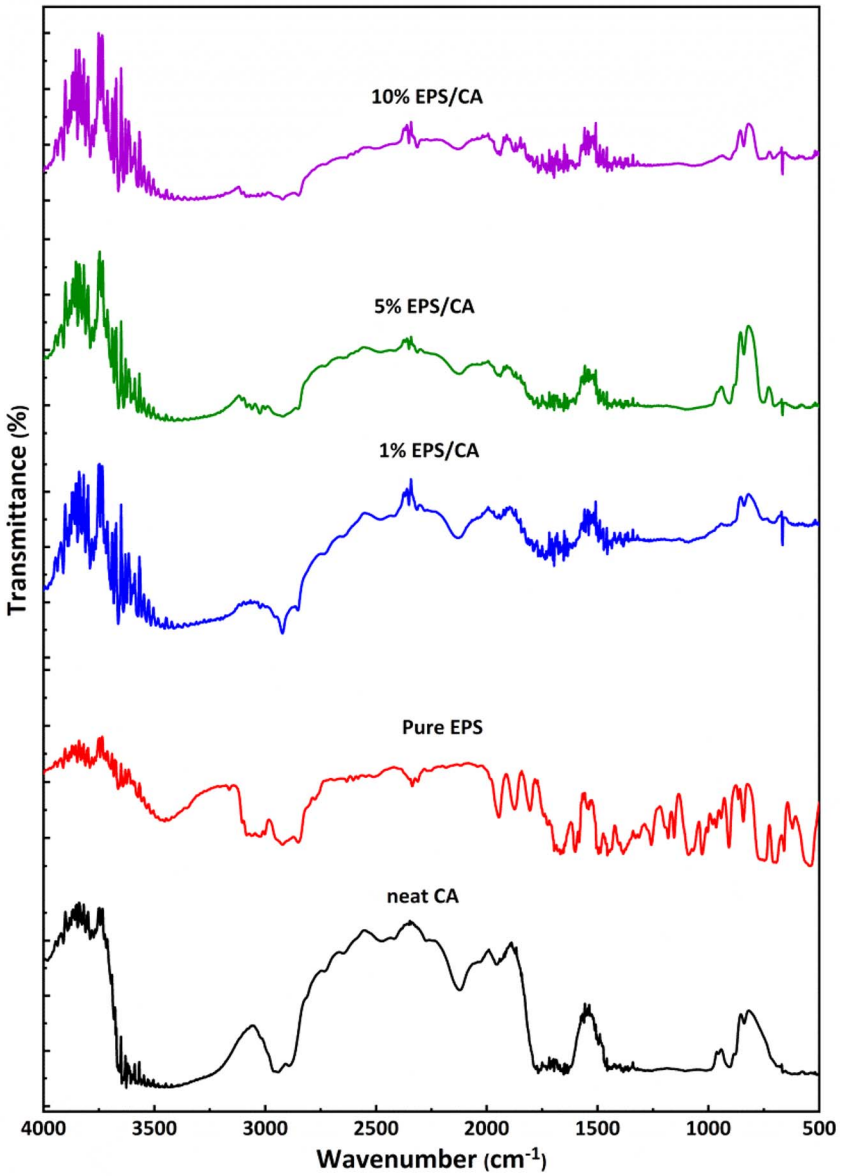

Fig. 3 FTIR spectrum of neat CA, EPS, and EPS/CA blend membranes.

contents with 1 wt%, 5 wt%, and 10 wt% is shown in Fig. 4. In the neat CA membrane's XRD pattern, a broad halo diffraction peak near 22.45° was detected which is due to semi-crystalline nature of CA.[27] This halo-like broad peak arises from the short range ordered regions in the amorphous matrix of cellulose. The absence of sharp crystalline peaks confirms that CA possesses predominantly amorphous characteristics. On the other hand, the XRD pattern of EPS showed a distinct broad peak at 19.5° corresponds to its amorphous structure. The pattern lacks in the sharp peaks which indicate absence of long range ordered chains within the polystyrene backbone. In case of EPS/CA blend membranes, the overall XRD pattern displayed characteristics of both CA and EPS with variations in the intensity and sharpness of the diffraction peaks. It was observed that the diffraction pattern of 1 wt% EPS/CA blend membrane is quite similar with the CA diffraction pattern with lower intensity showing a broad halo peak at 22.45°. This suggests that the lower loadings of EPS do not significantly affect the structure of overall polymer chains of CA, but it might create additional pathways for the gas to diffuse. As the EPS loading is increased to 5 wt% and 10 wt% in EPS/CA blend membranes a slight reduction in the intensity and broadening of the diffraction peak was observed that might be due to the incorporation of the amorphous EPS phase which disrupts the local packing of CA polymer chains. These structural changes may influence the transport properties of gas molecules through the polymer matrix.

3.4 DSC analysis

To determine the glass transition temperature (T_g) of the neat CA, EPS, and EPS/CA blend membranes DSC analysis was

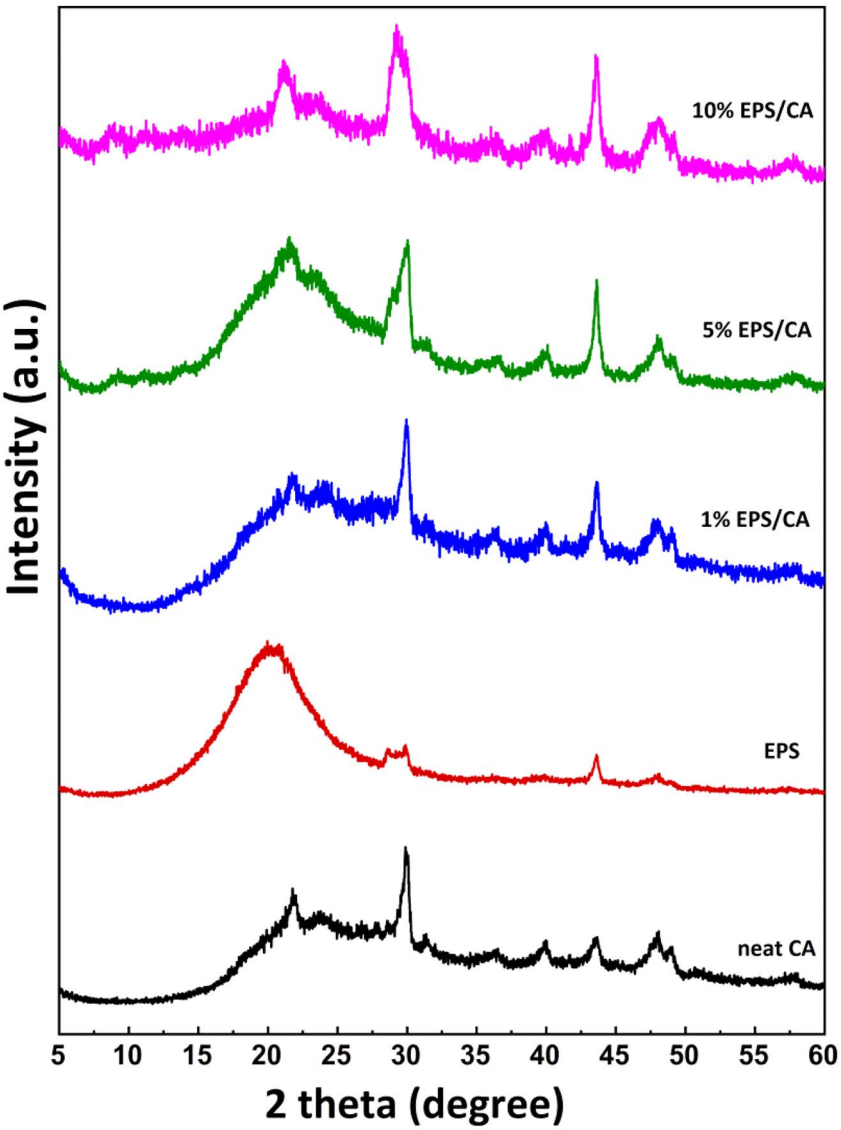

Fig. 4 XRD of neat CA, EPS, and EPS/CA blend membranes.

performed. The DSC measurements were performed under nitrogen atmosphere (20 ml min^{-1}), approximately 5 to 8 mg of sample mass was taken and the samples were heated from 25 °C to 250 °C at heating rate of 10 °C per minute. The analysis was conducted at least three times and the average values were reported to make sure reproducibility. The neat CA membrane showed a well defined T_g around 184 ± 0.52 °C which is consistent with the previously reported values for the CA membrane.[27] The high T_g is an indication of a rigid backbone of CA due to intermolecular interaction between acetate and hydroxyl groups. However, EPS showed a T_g around 98 ± 0.80 °C which corresponds to the segmental motion of amorphous polystyrene chains. As compared to CA the lower T_g of EPS indicates its softer and flexible nature. In case of EPS/CA blend membranes with increase in EPS content gradual decrease in T_g was observed. The 1 wt% EPS/CA blend displayed a T_g of 185 ± 0.72 °C which is nearly similar to neat CA indicating good miscibility. However, at 5 wt%, and 10 wt% EPS loadings the T_g was found to be 180 ± 0.54 °C and 175 ± 0.91 °C. The shifting in the T_g to lower temperatures indicates an increment in the polymer chain flexibility and enhanced free volume induced by the presence of softer EPS phase. This behavior supports the structural interpretation derived from both FTIR and XRD analysis where incorporation of EPS disrupts the ordered packing of CA and promotes amorphization.

3.5 FESEM analysis

The macroscopic images of neat CA, 1 wt% and 10 wt% of EPS are shown in Fig. 5a, d and g. It was observed that neat CA membrane appears transparent and more flexible. However, with increase in EPS loading, the EPS/CA blend membranes becomes non transparent and less flexible.

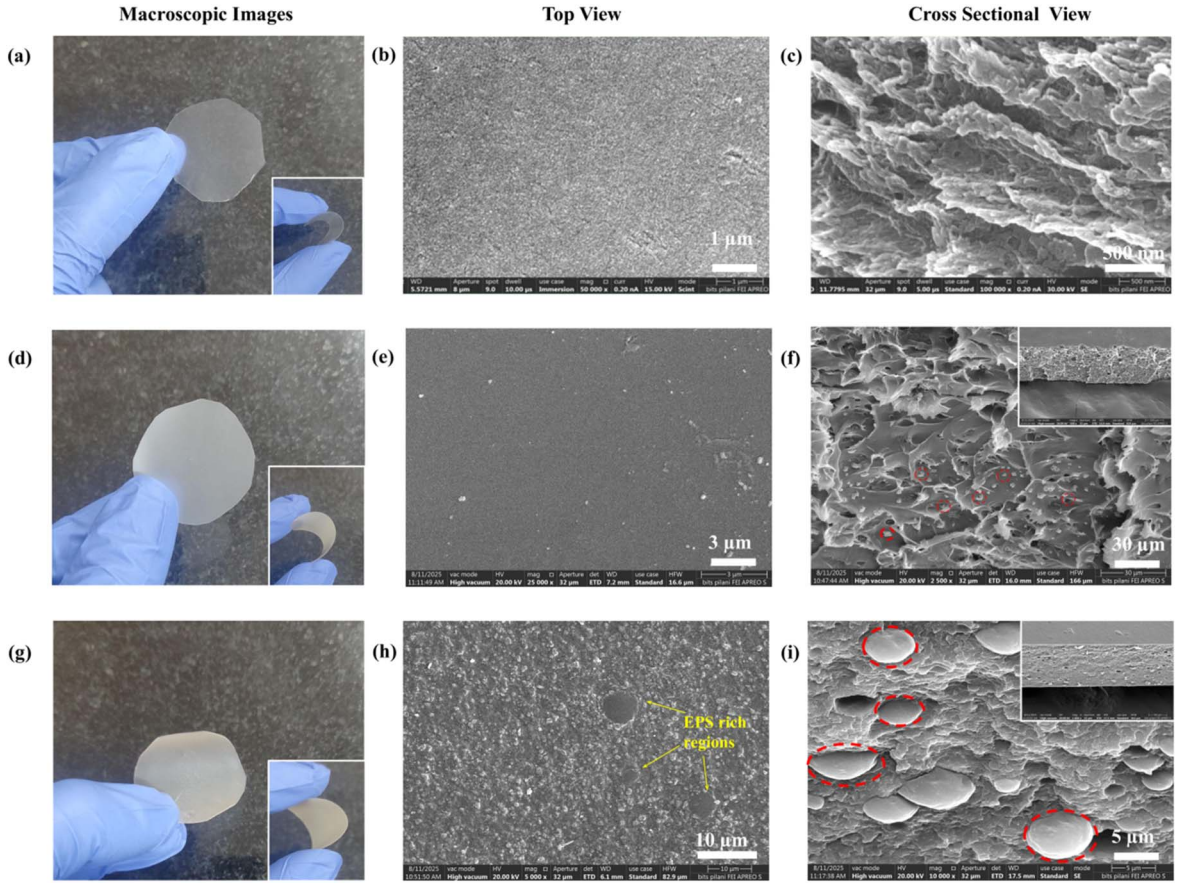

Fig. 5 Macroscopic and FESEM (top and cross-sectional) images of (a–c) neat CA, (d–f) 1% EPS/CA, and (g–i) 10% EPS/CA blend membranes.

To investigate the surface and cross-sectional morphologies of neat CA and EPS/CA blend membranes with 1 wt% and 10 wt% of EPS the FESEM technique was used (Fig. 4). In the FESEM image of neat CA membrane (Fig. 5b) the top surface looks defect free, smooth and homogeneous indicating the formation of a continuous polymer matrix. In the cross-sectional image (Fig. 5c), a non-porous compact structure with tightly packed polymer chains is visible. Such dense morphology is consistent with its amorphous character as also confirmed by XRD and the absence of crystallites could create voids or channels.

On the other hand, in case of EPS/CA blend membranes, at 1 wt% EPS loading the surface remained largely uniform and dense, similar to neat CA matrix. This confirms that interfacial adhesion and miscibility between CA at low loading of EPS. The EPS domains are finely dispersed within the CA matrix. Such morphology is indicative of intermolecular interaction (*e.g.* dipole–π interactions between acetyl and aromatic groups) which contributes to mechanical and thermal stability of the blend membrane. As EPS content was increased, slight roughness and microphase domains started to appear on the membrane surface. The dispersed EPS particles acted as micro barriers that disrupts the close packing of CA chains and increases the fractional free volume. This morphological change could facilitate CO_2 transport by creating additional pathways for permeation within the matrix while still maintaining overall membrane integrity. At 10 wt% EPS loading (Fig. 5h), the surface became more heterogeneous showing distinct EPS rich regions and interfacial boundaries. This indicates increase in phase separation due to reduced miscibility at higher EPS loading which results in dual phase morphology. Such morphology could enhance gas diffusivity due to increased free volume and micro voids due to which selectivity might reduce due to formation of non-selective transport regions. The cross-section image revealed a transition from a dense to slightly porous structure which aligns with the observed XRD results that indicates a reduction in ordering and increased amorphousness.

3.6 Tensile testing

In order to determine the mechanical properties of the neat CA membrane and investigate effect of EPS loading tensile testing was conducted (Fig. 6). Three samples of each membrane were tested to ensure reproducibility and average values were reported. The neat CA membrane showed a tensile strength of 9.51 MPa. On the introduction of 1% EPS a marginal decrease in the tensile strength was observed (5.89 MPa). This decline may be due to disruption in the tight packing of CA which is created by low loading of EPS inherent chains that may act as a spacer and decreases the overall resistance to mechanical

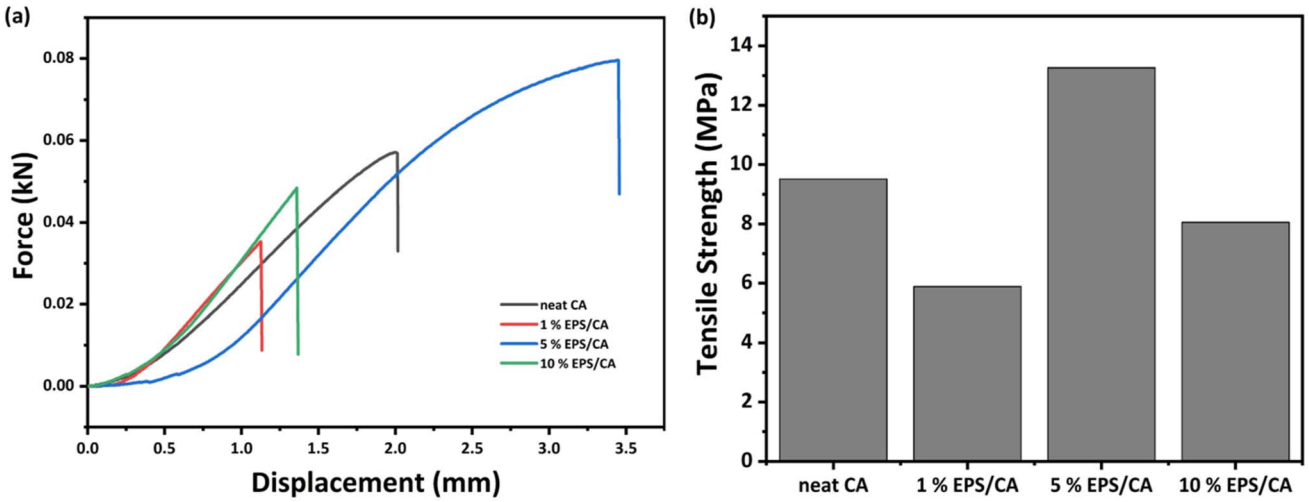

Fig. 6 Tensile testing of the neat CA, 1% EPS/CA, 5% EPS/CA, and 10% EPS/CA blend membranes at room temperature 25 °C (a) force *vs.* displacement curves, and (b) tensile strength.

deformation. 5% EPS loaded blend membrane showed highest tensile strength of 13.26 MPa. At this optimal loading, EPS molecules likely achieve uniform dispersion within CA matrix. The incorporation of EPS in CA matrix contributes to structural rigidity through effective stress transfer while maintaining flexibility. The tensile strength of 10% EPS loaded blend membrane reduced to 8.06 MPa falling below the strength of neat CA. This deterioration in mechanical properties at higher loading may be due to agglomeration of EPS. Excessive EPS concentration may lead to formation of molecular clusters that act as stress concentrators within polymer matrix. Such inhomogeneities disrupt the continuity of CA phase and facilitate crack propagation leading to premature failure under tensile load.

3.7 Gas permeation

The gas permeation behavior of neat CA, and EPS/CA blend membranes with 1 wt%, 5 wt%, and 10 wt% EPS loadings were conducted using a model CO_2/CH_4 biogas mixture (40 : 60) at two different pressures of 1.5 bar and 3 bar at 25 °C. To ensure the accuracy and repeatability of the results minimum three samples from each of the membranes under the same conditions were tested and their average values were reported. The permeabilities of CO_2 and CH_4 along with CO_2/CH_4 selectivity values are summarized in Table 1 and comparison graphs were plotted as shown in Fig. 7. Membrane sample having effective area of 3.14 cm^2 was used in the permeation cell. High purity nitrogen gas was used as sweep gas, and a back pressure regulator (BPR) was employed to maintain pressure and the permeate composition was analyzed using gas chromatography (Shimadzu GC-2014) equipped with thermal conductivity detector (TCD) detailed experimental conditions are present in the SI.

At 1.5 bar pressure, the neat CA membrane exhibited a CO_2 permeability of 6.44 ± 0.98 Barrer and a CH_4 permeability of 0.65 ± 0.06 Barrer, resulting in a CO_2/CH_4 selectivity of 20.79. The low gas permeability of neat CA membranes arises from its dense and semi-crystalline structure which was also confirmed by the XRD. The selectivity originates from the strong solubility of CO_2 in the polar acetyl groups *via* dipole–quadrupole interactions. When the EPS is introduced into the CA matrix the gas transport behavior of membranes was changed drastically. With 1 wt% EPS loading the CO_2 permeability increased nearly five times to 28.49 ± 1.35 Barrer while CH_4 permeability raised to 2.14 ± 0.07 Barrer leading to reduction in CO_2/CH_4 selectivity of 13.32. The increase in permeability can be attributed to the disruption of CA chain packing and the formation of additional free volume, as observed XRD results suggesting decrease crystallinity. The reduction in selectivity suggests that EPS

Table 1 Gas permeation at 1.5 and 3 bar pressure

	1.5 Bar pressure			3 Bar pressure		
Membrane	CH_4 permeability (Barrer)	CO_2 permeability (Barrer)	CO_2/CH_4 selectivity	CH_4 permeability (Barrer)	CO_2 permeability (Barrer)	CO_2/CH_4 selectivity
Neat CA	0.65 ± 0.06	6.44 ± 0.98	20.79 ± 0.91	0.77 ± 0.13	14.03 ± 0.25	18.06 ± 0.88
1% EPS/CA	2.14 ± 0.07	28.49 ± 1.35	13.32 ± 0.21	4.92 ± 0.86	63.14 ± 0.99	12.82 ± 0.96
5% EPS/CA	2.45 ± 0.6	45.50 ± 1.80	18.59 ± 1.86	6.22 ± 0.97	105.83 ± 1.12	15.98 ± 0.18
10% EPS/CA	2.28 ± 0.12	47.63 ± 1.05	21.25 ± 0.21	4.40 ± 0.24	76.78 ± 2.29	17.42 ± 0.61

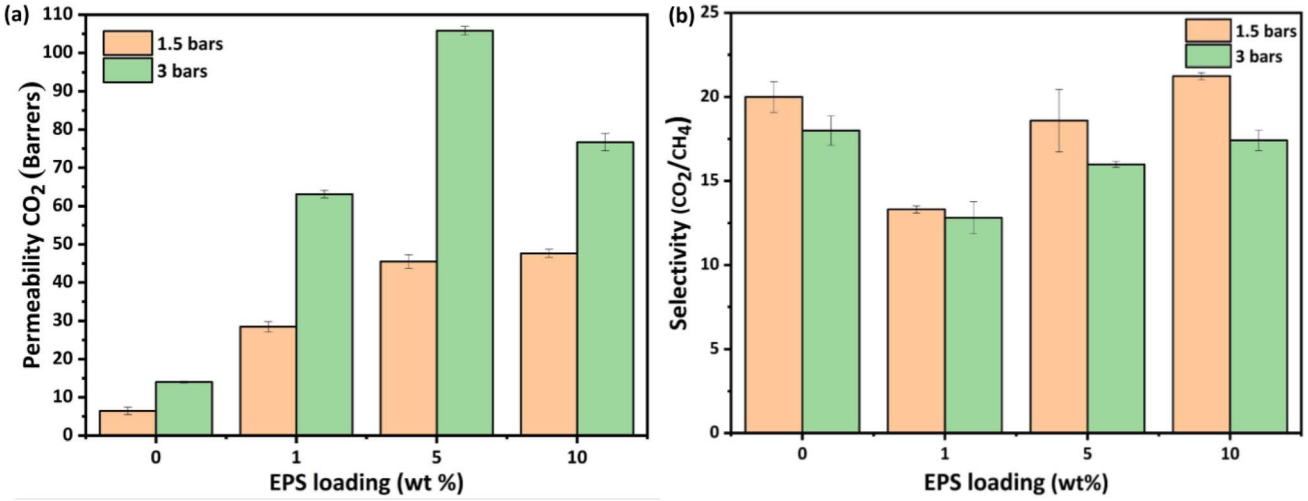

Fig. 7 Gas permeation results: (a) CO_2 permeability; (b) selectivity (CO_2/CH_4) of neat CA, 1% EPS/CA, 5% EPS/CA, and 10% EPS/CA blend membranes.

domains create less selective pathways for the transport of CO_2 and CH_4.

When the EPS loading increased to 5%, the CO_2 permeability also increased to 45.50 ± 1.80 Barrer along with CH_4 permeability of 2.45 ± 0.60 Barrer. The CO_2/CH_4 selectivity also increases to 18.59. At 10 wt% of EPS loading the CO_2 permeability further increased to 47.63 ± 1.05 Barrer with CH_4 permeability of 2.28 ± 0.12 Barrer and CO_2/CH_4 selectivity of 21.25. High EPS loading can induce partial phase separation which was also observed in FESEM that slight morphological heterogeneity generates microvoids and increases free volume that preferentially facilitate CO_2 diffusion and restores the selectivity to a level comparable to neat CA. This suggests dual-mode transport behavior where CO_2 permeates through both dense CA regions and EPS enriched domains.

At 3 bar pressure, all the membranes exhibited higher CO_2 and CH_4 permeabilities compared to 1.5 bars. For neat CA membrane the CO_2 permeability increased to 14.03 ± 0.25 Barrer and CH_4 to 0.77 ± 0.13 Barrer with a slight drop in selectivity to 18.06 which is typical dual mode sorption behavior where Langmuir sites become saturated at higher pressure. Similarly, for 1 wt% EPS/CA blend membrane the CO_2 permeability increases to 63.14 ± 0.99 Barrer and CH_4 permeability is 4.92 ± 0.86 Barrer with selectivity decreasing to 12.82. The 5 wt% EPS/CA blend membrane demonstrated excellent gas transport performance by achieving the highest CO_2 permeability of 105.83 ± 1.14 Barrer with CH_4 permeability of 6.22 ± 0.97 Barrer and a balanced selectivity of 15.98 that indicates its optimal phase morphology and polymer–polymer compatibility. For 10 wt% EPS/CA blend membrane, the measured CO_2 permeability was 76.78 ± 2.29 Barrer and CH_4 permeability was 4.40 ± 0.24 Barrer with a selectivity of 17.42. This suggests that high EPS loading results in minor phase separation and non-selective microvoids that increases permeability but limits selectivity enhancement.

The polar acetyl groups present in the cellulose acetate enhances the CO_2 solubility through dipole–quadrupole interactions. Due to incorporation of EPS, the aromatic polystyrene domain disrupts the CA chain packing and increases the fractional free volume. This change in the structure facilitates faster gas diffusion. At moderate EPS loading (5 wt%), optimal permeability is observed due to the balance between increased free volume and maintained polymer compatibility. Whereas at 10 wt% loading, partial phase separation leads to microvoids formation which can increase diffusivity but may reduces the selectivity.

The fabricated EPS/CA blend membranes gas separation capacity was compared with various available literatures on polymer blend membranes for CO_2/CH_4 separation (Table 2). The Pebax-1657/PDMS–PEO blend have shown high CO_2 permeability of 1629 Barrer but low selectivity of 10.1 which is due to flexible PDMS and PEO domains that facilitate rapid gas diffusion.[28] Similarly, Pebax/PEG and Pebax-1657/PAMAM blends showed CO_2 permeability of 56.9 and 63.1 Barrer with moderate selectivity of 13 and 23.6, respectively.[29,30] On the other hand, PSf/PEI, PSf/PBS, and SPEEK/PEI polymer blends showed lower CO_2 permeability of 7.62, 14.17, and 48 Barrer with 13, 33, and 15 selectivity.[21,31,32] This comparatively high selectivity of these blends was due to the rigid aromatic backbone and lower fractional free volume. Cellulose based blends such as PSf/CTA and CTA/CDA have reported moderate permeabilities (11–17 Barrers) and selectivities (18–31) arising from the polar acetate functionality that enhances CO_2 solubility.[33,34] In comparison, the developed EPS/CA blend membranes in this work have shown excellent trade-off between permeability and selectivity. At 1.5 bars, the 10 wt% EPS/CA membrane showed CO_2 permeability of 47.63 Barrer with a CO_2/CH_4 selectivity of 21.25. Whereas, at 3 bars the 5 wt% EPS/CA membrane showed 105.83 Barrer CO_2 permeability with 15.98 selectivity. These values are notably higher than many reported CA based or polysulfone based blends such as CA/PI

Table 2 Comparison of EPS/CA blend membranes gas separation capacity with various available literatures on polymer blend membranes for CO_2/CH_4 separation

Blend membranes	Gas pairs	CO_2 permeability	Selectivity	Testing conditions	Ref.
Cellulose acetate (CA)/polyimide (PI)	CO_2/CH_4	19.71 Barrer	9.42	1.5 Bar 25 °C	20
Cellulose triacetate (CTA)/cellulose diacetate (CDA)	CO_2/CH_4	17.32 Barrer	18.55	5 Bar 25 °C	34
Cellulose acetate (CA)/expanded polystyrene (EPS) (5 wt%)	CO_2/CH_4	47.63 Barrer	21.25	1.5 Bar 25 °C	This work
Cellulose acetate (CA)/expanded polystyrene (EPS) (10 wt%)	CO_2/CH_4	105.83 Barrer	15.98	3 Bar 25 °C	This work
Polysulfone (PSf)/poly(butylene succinate) (PBS)	CO_2/CH_4	14.172 GPU	33	3 Bar 27 °C	21
Polysulfone (PSF)/poyetherimide (PEI)	CO_2/CH_4	7.62 Barrer	13.06	10 Bar 25 °C	31
Polysulfone (PSf)/cellulose triacetate (CTA)	CO_2/CH_4	11.12 Barrer	30.70	4 Bar 25 °C	33
Poly(ether-*block*-amide) (Pebax-1657)/ polydimethylsiloxane–polyethylene oxide (PDMS–PEO)	CO_2/CH_4	1629 Barrer	10.1	~2 Bar 25 °C	28
Poly(ether-*block*-amide) (PEBAX)/ polyethylene glycol (PEG)	CO_2/CH_4	63.12 Barrer	23.6	7 Bar 25 °C	29
Poly(ether-*b*-amide) (Pebax-1657)/ poly(amidoamine) (PAMAM)	CO_2/CH_4	56.9 Barrer	13	2 Bar 30 °C	30
Poly(ether ether ketone) (SPEEK)/ polyetherimide (PEI)	CO_2/CH_4	48 Barrer	15	2 Bar 35 °C	32
Polyurethane (PU)/nylon 6(3)	CO_2/CH_4	16.1 Barrer	18.95	8 Bar 25 °C	35
Polyurethane (PU)/ poly(methylmethacrylate) (PMMA)	CO_2/CH_4	33.6 Barrer	11.77	1.6 Bar 25 °C	36

(19.71 Barrer, 9.42), PSf/CTA (11.12 Barrer, 30.7), and CTA/CDA (17.32 Barrer, 18.55).[20,33,34] The EPS/CA blend membranes compared with the other polymer blend systems that contain highly flexible polymers (for example PDMS) show very high permeability but poor selectivity due to excessive chain mobility. On the other hand, the rigid aromatic polymer system like PSF/PEI membranes shows higher selectivity but lower permeability due to reduced fractional free volume. Therefore, the EPS/CA blends membrane provide a balanced structure in which EPS increases the free volume while CA retains polar functional groups that enhances CO_2 sorption.

4 Conclusion

A series of EPS/CA blend membranes were developed in this study by varying EPS loading through solution casting and solvent evaporation technique. The membranes were tested with the model biogas mixture having a composition of CO_2 and CH_4 in a 40 : 60 ratio at two different pressures of 1.5 and 3 bar. Structural and thermal analyses confirmed the formation of physically compatible blends without the formation of new chemical bonds. FTIR spectra revealed the coexistence of functional groups from both CA and EPS. XRD analysis indicated a reduction in CA's semi-crystallinity with increase in EPS content that shows improvement in chain mobility and interfacial interaction between the two polymers. The DSC analyses demonstrated that the incorporation of EPS reduced the glass transition temperature of the blends. In FESEM analysis smooth and defect free surfaces at lower EPS loadings (1 wt%) was observed. At higher loading of EPS (10 wt%) phase separation became apparent which indicates limited compatibility beyond a threshold concentration. Gas permeation studies showed that the 5 wt% EPS loaded blend membrane has shown highest CO_2 permeability of 105.83 Barrer at 3 bars. Also, at 1.5 bars, the 10 wt% EPS blend membrane has shown highest the CO_2/CH_4 selectivity of 21.25 with enhanced CO_2 permeability 47.63 Barrer. The obtained results have demonstrated that blending waste EPS with CA offers a sustainable approach that improves the performance of the polymeric membranes for CO_2/CH_4 separation. Although the membrane approaches the upper bound it does not surpass it. This limitation may arise due to partial miscibility between CA and EPS, or formation of microvoids at higher EPS loadings, and absence of highly selective molecular sieving structures. Therefore, to tackle these limitations in future work, functional nanofillers like MOFs or graphene derivatives will be incorporated in the blends. This strategy of upcycling of non-biodegradable waste EPS into functional membrane material aligns with circular economy principles and provides a new path to develop environment friendly membranes which can be used to upgrade biogas. Despite the promising results obtained in the present study several limitations were observed which will be focused in future investigation. Firstly, the long term operational stability of CA/EPS membranes under continuous gas separation conditions. Another will be scalability of the fabrication process for industrial membrane production. As the present study focussed on utilization of waste EPS as membrane material for mixed gas separation under controlled conditions. Further investigation will evaluate the membrane's performance under

real biogas conditions to address the practical applicability in large scale biogas upgrading processes.

Author contributions

BN carried out conceptualization, methodology, investigation, data curation, and writing – original draft. MG contributed in material synthesis and data analysis. BVRK was involved in conceptualization, methodology, formal analysis, writing – review, editing, and supervision.

Conflicts of interest

The authors declare that they have no known competing financial interests or personal relationships that could have appeared to influence the work reported in this paper.

Data availability

The authors declare that the data supporting the findings of this study are available within the paper.

Supplementary information (SI) is available. See DOI: https://doi.org/10.1039/d6ra01412g.

References

1 M. A. Fayshal, *Heliyon*, 2024, **10**, e40838.
2 Y. K. Song, S. H. Hong, S. Eo, G. M. Han and W. J. Shim, *Environ. Sci. Technol.*, 2020, **54**, 11191–11200.
3 S. C. H. Mangalara and S. Varughese, *ACS Sustain. Chem. Eng.*, 2016, **4**, 6095–6100.
4 S. Santana-Luna, M. Yam-Cervantes, R. Sulub-Sulub, M. Huhn-Ibarra, H. Vázquez, S. Duarte, W. Herrera-Kao and M. O. González-Díaz, *ACS Sustain. Chem. Eng.*, 2025, **13**, 17939–17948.
5 Y. Li, C. P. Alaimo, M. Kim, N. Y. Kado, J. Peppers, J. Xue, C. Wan, P. G. Green, R. Zhang, B. M. Jenkins, C. F. A. Vogel, S. Wuertz, T. M. Young and M. J. Kleeman, *Environ. Sci. Technol.*, 2019, **53**, 11569–11579.
6 X. Y. Chen, H. Vinh-Thang, A. A. Ramirez, D. Rodrigue and S. Kaliaguine, *RSC Adv.*, 2015, **5**, 24399–24448.
7 A. Soliman, N. Alamoodi, G. N. Karanikolos, C. C. Doumanidis and K. Polychronopoulou, *Nanomaterials*, 2020, **10**, 1–38.
8 R. Sholl and D. Lively, *Nature*, 2016, **532**, 435–437.
9 A. M. Varghese and G. N. Karanikolos, *Int. J. Greenh. Gas Control*, 2020, **96**, 103005.
10 W. J. Koros and G. K. Fleming, *J. Membr. Sci.*, 1993, **83**, 1–80.
11 R. Sidhikku Kandath Valappil, N. Ghasem and M. Al-Marzouqi, *J. Ind. Eng. Chem.*, 2021, **98**, 103–129.
12 L. M. Robeson, *Curr. Opin. Solid State Mater. Sci.*, 1999, **4**, 549–552.
13 A. Roozitalab, A. Kargari and M. Soleimani, *Environ. Technol. Innov.*, 2025, **40**, 104557.
14 G. Di Luca, F. Galiano, F. Russo, S. Tornaghi, E. Di Nicolò, R. Mancuso, B. Gabriele and A. Figoli, *ACS Sustain. Chem. Eng.*, 2025, **13**, 9074–9086.
15 R. Lettieri, A. Caravella, G. Quintarelli, C. D'Ottavi, S. Licoccia and E. Gatto, *ACS Sustain. Chem. Eng.*, 2025, **13**, 16178–16191.
16 Z. Bashir, S. S. M. Lock, N. e. Hira, S. U. Ilyas, L. G. Lim, I. S. M. Lock, C. L. Yiin and M. A. Darban, *RSC Adv.*, 2024, **14**, 19560–19580.
17 P. Tanvidkar, A. Jonnalagedda and B. V. R. Kuncharam, *Environ. Technol.*, 2024, **45**, 2867–2878.
18 G. Dong, H. Li and V. Chen, *J. Mater. Chem. A*, 2013, **1**, 4610–4630.
19 T. M. Neves, L. D. Pollo, N. R. Marcilio and I. C. Tessaro, *Polym. Bull.*, 2025, **82**, 12869–12891.
20 B. Nayak, P. Tanvidkar and B. V. R. Kuncharam, *Polym. Eng. Sci.*, 2024, **64**, 788–797.
21 S. Payami, M. Pourafshari Chenar and M. R. Moradi, *J. Appl. Polym. Sci.*, 2025, **142**, 1–12.
22 Z. Niu, N. He, Y. Yao, A. Ma, E. Zhang, L. Cheng, Y. Li and X. Lu, *Chem. Eng. J.*, 2024, **494**, 152912.
23 P. Tanvidkar, B. Nayak and B. V. R. Kuncharam, *J. Polym. Environ.*, 2023, **31**, 3404–3417.
24 L. Yan and J. Wang, *Desalination*, 2011, **281**, 455–461.
25 Y. Zhou, Y. Jiang, Y. Zhang and L. Tan, *ACS Appl. Mater. Interfaces*, 2022, **14**, 38358–38369.
26 E. Jansri, N. Roungpaisan, S. Pivsa-Art and P. Kampeerapappun, *ACS Sustain. Chem. Eng.*, 2025, **13**, 1788–1797.
27 B. Nayak and B. V. R. Kuncharam, *Polym. Eng. Sci.*, 2024, **65**, 6265–6277.
28 C. Z. Liang, F. Feng, J. Wu and T. S. Chung, *J. Membr. Sci.*, 2025, **716**, 123528.
29 P. Taheri, A. Raisi and M. S. Maleh, *Environ. Sci. Pollut. Res.*, 2021, **28**, 38274–38291.
30 A. Tayebi, A. Kargari and S. Akbari, *Polym. Test.*, 2023, **128**, 108225.
31 H. Mukhtar, H. A. Mannan, D. Minh, R. Nasir, D. F. Moshshim and T. Murugesan, *IOP Conf. Ser. Earth Environ. Sci.*, 2016, **36**, 12016.
32 H. Bahreini, E. Ameri and H. Ebadi-Dehaghani, *Arab. J. Chem.*, 2024, **17**, 105400.
33 H. Roafi, S. Farrukh, Z. Salahuddin, A. Raza, S. S. Karim and H. Waheed, *J. Polym. Environ.*, 2024, **32**, 2414–2430.
34 A. Raza, S. Farrukh, A. Hussain, I. Khan, M. H. D. Othman and M. Ahsan, *Membranes*, 2021, **11**, 245.
35 S. Kiani and A. Raisi, *J. Appl. Polym. Sci.*, 2022, **139**, e52812.
36 J. A. de Sales, P. S. O. Patrício, J. C. Machado, G. G. Silva and D. Windmöller, *J. Membr. Sci.*, 2008, **310**, 129–140.